

# Study on $\text{Sm}^{3+}$ and $\text{Er}^{3+}$ Co-Doped $\text{CeO}_2$ -Based Electrolytes

A. ARABACI\*

Istanbul University, Faculty of Engineering, Department of Metallurgical and Materials Engineering,  
Avcilar, 34320 Istanbul, Turkey

Ceria doped with aliovalent cations, such as rare earth oxides, has been considered as one of the most promising candidate electrolyte materials for intermediate temperature solid oxide fuel cells. In this study, high purity cerium nitrate, samarium nitrate and erbium nitrate salts were used to obtain ceria-based solid solutions  $\text{Ce}_{0.80}\text{Sm}_{0.20}\text{O}_{1.90}$  (SDC),  $\text{Ce}_{0.80}\text{Sm}_{0.15}\text{Er}_{0.05}\text{O}_{1.90}$  (ESDC5),  $\text{Ce}_{0.80}\text{Sm}_{0.10}\text{Er}_{0.10}\text{O}_{1.90}$  (ESDC10) through the cellulose templating method. Crystal structure and microstructure were characterized by means of X-ray diffraction and scanning electron microscopy, respectively. X-ray diffraction results indicate that a single-phase fluorite structure formed at a relatively low calcination temperature, 500 °C. The relative densities of the sintered pellets were higher than 93%. The electrical properties of doped and co-doped ceria electrolytes in the temperature range 300–750 °C were analyzed by using electrochemical impedance spectroscopy. The singly doped ceria at 750 °C showed the highest ionic conductivity with less activation energy.

DOI: [10.12693/APhysPolA.132.458](https://doi.org/10.12693/APhysPolA.132.458)

PACS/topics: electrical conductivity, electrolyte material, the cellulose templating (CT) method, co-doped ceria

## 1. Introduction

Nowadays, several studies are being carried out on developing clean and renewable energy sources such as wind energy, solar energy, etc. to protect the ecosystem [1–5]. Among the alternative energy sources, fuel cells draw much more attention. Fuel cell is an electrochemical device that directly converts the chemical energy of a fuel into electrical energy. It is made up of two electrodes, each coated with a catalyst, separated by an electrolyte. Electrolytes used for fuel cells are usually the main components for determining the performance of the cell. Ceria doped with aliovalent cations, such as rare earth oxides, has been considered as one of the most promising candidate electrolyte materials for intermediate temperature solid oxide fuel cells (ITSOFCs) [6, 7]. These materials show much higher ionic conductivity at relatively lower temperatures than the traditional electrolyte yttria-stabilized zirconia (YSZ). Until now, many studies have been carried out about doped ceria and significant progress have been obtained [8–11]. Some singly doped electrolytes, such as  $\text{Ce}_{1-x}\text{Sm}_x\text{O}_{2-y}$  and  $\text{Ce}_{1-x}\text{Gd}_x\text{O}_{2-y}$  demonstrate high oxide ion conductivity [6, 7], but the SOFCs based on those have not met the commercial requirement so far. With the purpose of optimizing electrolyte materials further, co-doping method has been used recently. For example,  $\text{Ce}_{1-x-y}\text{La}_x\text{Sr}_y\text{O}_{2-z}$  [12],  $\text{Ce}_{1-a}\text{Gd}_{a-y}\text{Sm}_y\text{O}_{2-0.5a}$  [13],  $\text{Ce}_{0.85}\text{Gd}_{0.1}\text{Mg}_{0.05}\text{O}_{1.9}$  [14], so on. However, there is still a lack of systematic studies reported on various dopant types.

In this study, a set of Sm and Er co-doped ceria electrolytes were prepared and characterized. The effect of

co-doping on the crystal structure and electrical conductivity was studied in comparison to singly doped ceria ( $\text{Ce}_{0.80}\text{Sm}_{0.20}\text{O}_{1.90}$ ). The purpose is to develop new ceria-based electrolyte materials with better properties for ITSOFCs.

## 2. Materials and methods

A series of samples with the general formula  $\text{Ce}_{0.80}\text{Sm}_{0.20}\text{O}_{1.90}$  (SDC),  $\text{Ce}_{0.80}\text{Sm}_{0.15}\text{Er}_{0.05}\text{O}_{1.90}$  (ESDC5),  $\text{Ce}_{0.80}\text{Sm}_{0.10}\text{Er}_{0.10}\text{O}_{1.90}$  (ESDC10) were prepared by the cellulose templating (CT) method using  $\text{Ce}(\text{NO}_3)_3 \cdot 6\text{H}_2\text{O}$  (Sigma-Aldrich, 99.999%),  $\text{Sm}(\text{NO}_3)_3 \cdot 6\text{H}_2\text{O}$  (Sigma-Aldrich, 99.999%) and  $\text{Er}(\text{NO}_3)_3 \cdot 5\text{H}_2\text{O}$  (Sigma-Aldrich, 99.99%) salts as the starting materials. Further detail about the CT method can be obtained from our earlier work [15]. For fabricating an electrolyte, the powders calcined at 500 °C for 4 h were uniaxially pressed (10 MPa) into disc-shaped pellets and subsequently isostatically pressed at 200 MPa. The shaped samples were sintered at 1400 °C for 6 h in air. The apparent densities of the sintered pellets were determined considering the Archimedes principle where water was used as the solvent (water at 25 °C 0.997 g/cm<sup>3</sup>) [16].

The crystal structures of the calcined powders were investigated by X-ray diffraction (XRD) analysis employing a Rigaku D/Max-2200 PC, monochromated  $\text{Cu } K_\alpha$  radiation,  $\lambda = 0.15418$  nm) at room temperature, in the Bragg angle range of  $10^\circ \leq 2\theta \leq 90^\circ$ . The crystallite sizes of the calcined powders were estimated according to the Scherrer formula [15].

The morphological characteristics of the sintered pellets were examined using scanning electron microscopy (SEM) (FEI-QUANTA FEG 450). Impedance measurements (electrochemical impedance spectroscopy (EIS)) were conducted with the SOLARTRON 1260 FRA branded device and 1296 interface at temperature ranges

\*e-mail: [aliye@istanbul.edu.tr](mailto:aliye@istanbul.edu.tr)

between 300 and 750 °C in air atmosphere. Before performing the impedance measurements, silver paste was brushed to each side of the samples, which was subsequently dried (at 800 °C for 30 min) enabling solid silver electrode on both sides of the pellet.

### 3. Results and discussion

#### 3.1. Crystal structures

Figure 1a illustrates the X-ray diffraction spectra of three powder samples calcined at 500 °C for 4 h and Fig. 1b exhibits the X-ray diffraction spectrum of pure  $\text{CeO}_2$ . No other peaks were detected, which proves that  $\text{Sm}_2\text{O}_3$  and  $\text{Er}_2\text{O}_3$  was completely dissolved in the  $\text{CeO}_2$  lattice forming a solid solution with the cubic  $\text{CeO}_2$  (JCPDS Card No:34-0394) structure. These results indicate that the doped ceria samples are all solid solutions of fluorite type structures that were formed due to the calcining process.

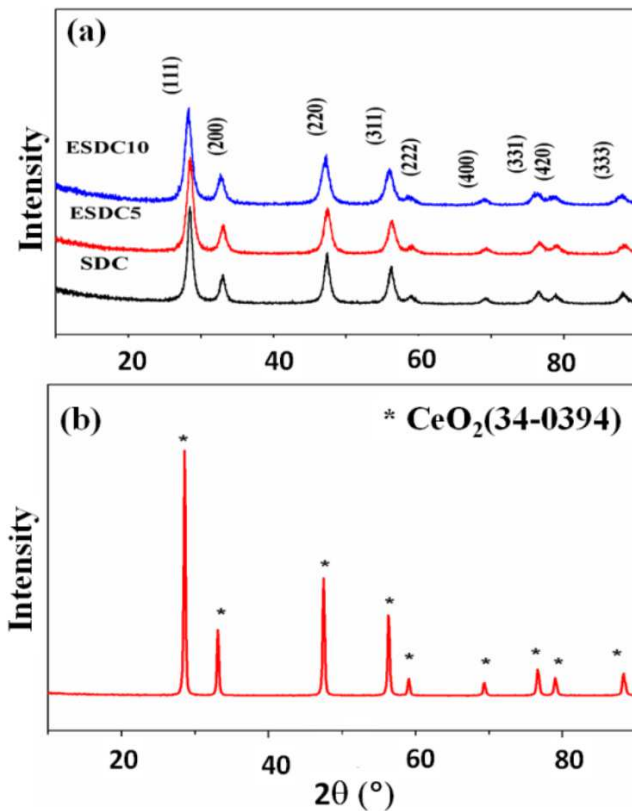


Fig. 1. Powder X-ray diffraction patterns of (a) SDC, ESDC5, and ESDC10 solid solutions and (b) pure  $\text{CeO}_2$ .

The addition of  $\text{Sm}^{3+}$  and  $\text{Er}^{3+}$  into  $\text{Ce}^{4+}$  can cause a small shift toward lower angle in the pure ceria peaks. This is because of the larger ionic radius of the samarium ion (0.109 nm) and erbium ion (0.1004 nm) compared to that of the cerium ion (0.097 nm). This indicates that samarium and erbium dissolved into the Ce sites in the SDC, ESDC5, ESDC10 systems.

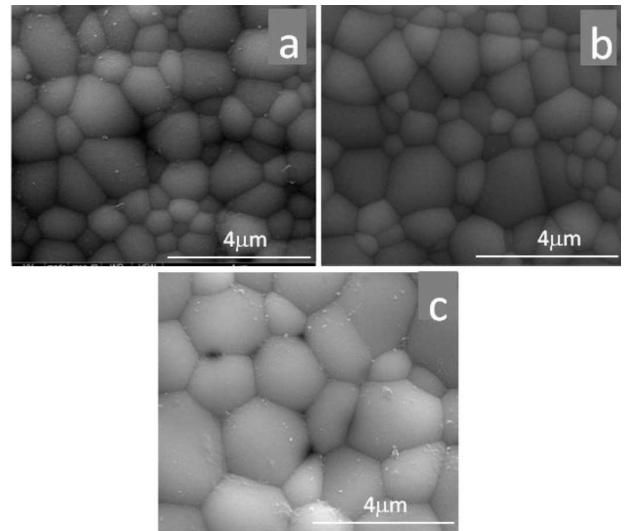


Fig. 2. SEM photographs of the sintered samples at 1400 °C for 6 h in air: (a) SDC, (b) ESDC5 and (c) ESDC10 ( $\times 30,000$ ).

The average crystallite sizes of the calcined powders calculated by the Scherrer formula and found as 13, 14.7, and 16 nm for SDC, ESDC5, and ESDC10, respectively.

Figure 2 shows the SEM images of the SDC, ESDC5, and ESDC10 samples. It is clearly seen that the surfaces of the samples are highly dense. This is in good agreement with the relative density values of the samples. The relative densities of the sintered pellets were measured over 93%. The sintered densities of all samples were determined by using the Archimedes principle [15]. It can also be seen that as the Er content is increased, grain structure had become coarser. The corresponding average grain size measurements are 1.06, 1.14, and 1.84  $\mu\text{m}$  for SDC, ESDC5, and ESDC10. Solute impurities such as  $\text{Er}^{3+}$  and  $\text{Sm}^{3+}$  may cause vacancy or strain energy regions in the ceria lattice. As  $\text{Er}^{3+}$  ions increase in the crystal lattice, this may result in internal stress or vacancy. Thus, at a high temperature (1400 °C), mobility of ions may increase and thereby grain growth may enhance.

#### 3.2. Electrical conductivity

The sample total resistance,  $R_T$  can be obtained by utilizing the impedance spectroscopy at different temperatures. The total electrical conductivity  $\sigma_T$  was then calculated according to the equation,

$$R_T = R_{\text{grain}} + R_{\text{grain-boundary}} \quad (1)$$

The total electrical conductivity  $\sigma_T$  was then determined from the equation

$$\sigma_t = l/AR_T, \quad (2)$$

where  $l$  is the thickness and  $A$  is the cross-sectional area of the sample.

SOFC electrolytes (such as yttria stabilized zirconia (YSZ), doped ceria) are oxygen ion conductors. It was

documented that the main contribution of the conductivity of ceria based electrolytes in air was the ionic conductivity and the contribution of electronic conductivity was negligible [7, 17]. In this study, the conductivity measured in air was treated as the oxide ionic conductivity only.

The ionic conductivity ( $\sigma_t$ ) in these oxides is a thermally activated process. Temperature dependence of the ionic conductivity can be expressed by the following empirical relationship:

$$\sigma_t T = \sigma_0 \exp\left(-\frac{E_a}{kT}\right), \quad (3)$$

where  $E_a$  is the activation energy for conduction,  $T$  is the absolute temperature,  $k$  is the Boltzmann constant and  $\sigma_0$  is a pre-exponential factor. The equation can be linearised by plotting a logarithmic relationship between  $\log(\sigma_t T)$  and  $1000/T$ .

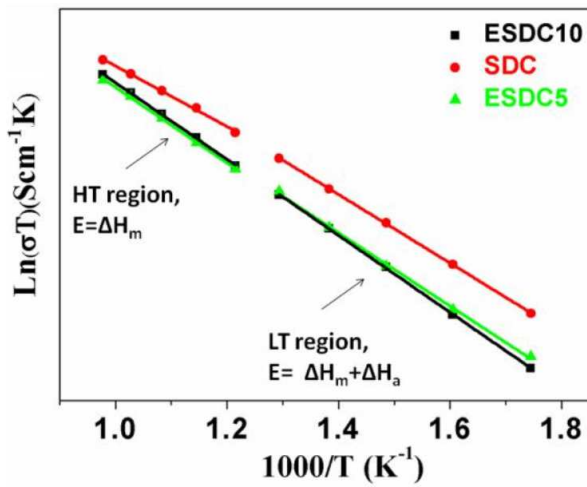


Fig. 3. The Arrhenius plots for total ionic conductivity of SDC, ESDC5 and ESDC10 samples.

The doping of trivalent oxides ( $\text{Sm}^{3+}$ ) into ceria creates oxygen vacancies, which are responsible for the ionic conduction in these oxides [7]. From Fig. 3 it can be seen that the conductivities of samarium and erbium co-doped ceria are lower than the single-doped ceria (SDC). The activation energies of SDC, ESDC5, ESDC10 samples are 0.79, 0.98, 1.01 eV, respectively. The change in the activation energy may be attributed to an order and disorder transition of the oxygen sublattice [7]. The activation energy is minimum for the SDC. This decrease in activation energy may be due to the presence of attractive interactions between dopant cations and oxygen vacancies [6, 7]. Furthermore, an increase in the Er dopant content for the  $\text{Ce}_{0.80}\text{Sm}_{0.20-x}\text{Er}_x\text{O}_{1.90}$  ( $x = 0.0, 0.05, 0.10$ ) system, co-dopant process hinders oxygen arrangement causing an increase in the activation energy and a decrease in the ionic conductivity for the ceria solid solutions.

Moreover, activation energy ( $E_a$ ) is the sum of the defect association enthalpy ( $\Delta H_a$ ) and migration enthalpy ( $\Delta H_m$ ) for conduction. At lower temperatures, acti-

vation energy depends on these two contributions. At higher temperatures, activation energy is equal to only the migration enthalpy ( $\Delta H_m$ ), because a great part of the oxygen vacancies are free to diffuse [6, 7].

#### 4. Conclusions

The single-phase fluorites SDC, ESDC5, ESDC10 were prepared by the cellulose templating (CT) method. All crystallite powders that were calcined at 500 °C for 4 h had a cubic fluorite structure and the average crystallite size was between 13 and 16 nm. The pellets were then sintered at 1400 °C in air atmosphere for 6 h. The relative densities of these pellets were over 93%. This result is in good agreement with the SEM images. The impedance measurements were performed in an open circuit using two electrode configurations. The results showed that  $\text{Ce}_{0.8}\text{Sm}_{0.2}\text{O}_{1.9}$  had the highest electrical conductivity,  $\sigma_{750^\circ\text{C}}$ , which is equal to  $3 \times 10^{-2} \text{ S cm}^{-1}$  and the lowest activation energy was found as equal to 0.79 eV. It can be concluded that co-doping with the rare-earth cation  $\text{Er}^{3+}$  has reduced the electrical properties of samarium doped ceria electrolytes (singly doped ceria).

#### References

- [1] S.S. Yegeubayeva, A.B. Bayeshov, A.K. Bayeshova, *Acta Phys. Pol. A* **128**, 455 (2015).
- [2] A.A. Jadallah, D.Y. Mahmood, Z. Er, Z.A. Abdulqaedr, *Acta Phys. Pol. A* **130**, 434 (2016).
- [3] Z. Er, *Acta Phys. Pol. A* **128**, 477 (2015).
- [4] O.M. Pişirira, O. Bingöl, *Acta Phys. Pol. A* **130**, 36 (2016).
- [5] B. Kiriş, O. Bingöl, R. Şenol, A. Altıntaş, *Acta Phys. Pol. A* **130**, 55 (2016).
- [6] B.C.H. Steele, *Solid State Ion.* **129**, 95 (2000).
- [7] H. Inaba, H. Tagawa, Ceria-Based Solid Electrolytes, *Solid State Ion.* **83**, 1 (1996).
- [8] S.K. Tadokoro, E.N.S. Muccillo, *J. Alloys Comp.* **374**, 190 (2004).
- [9] C. Peng, Y. Wang, K. Jiang, B.Q. Bin, H.W. Liang, J. Feng, J. Meng, *J. Alloys Comp.* **349**, 273 (2003).
- [10] S.W. Zha, C.R. Xia, G.Y. Meng, *J. Power Sourc.* **115**, 44 (2003).
- [11] D.Y. Chung, E.H. Lee, *J. Alloys Comp.* **374**, 69 (2004).
- [12] T. Mori, J. Drennan, J.H. Lee, J.G. Li, T. Ikegami, *Solid State Ion.* **154-155**, 461 (2002).
- [13] F.Y. Wang, B.Z. Wan, S. Chen, *J. Solid State Electrochem.* **9**, 168 (2005).
- [14] F. Wang, S. Chen, Q. Wang, S. Yu, S. Cheng, *Catal. Today* **97**, 189 (2004).
- [15] A. Arabacı, Ö. Serin, *J. Mater. Eng. Perform.* **24**, 2730 (2015).
- [16] A. Arabacı, Ö. Serin, *Acta Phys. Pol. A* **128**, B-118 (2015).
- [17] W. Lai, S.M. Haile, *J. Am. Ceram. Soc.* **88**, 2979 (2005).